Original Article
Establishment of pancreatic cancer patient-derived xenograft models and comparison of the differences among the generations

Wei Xu[1], Xiao-Wei Yang[1,2], Zheng-Yun Zhao[3], Bin Dong[4], Xiao-Ya Guan[1], Xiu-Yun Tian[1], Hong-Gang Qian[1], Chun-Yi Hao[1]

[1]Key Laboratory of Carcinogenesis and Translational Research (Ministry of Education), Department of Hepato-Pancreato-Biliary Surgery, Peking University Cancer Hospital & Institute, No. 52 Fucheng Road, Haidian District, Beijing 100142, China; [2]Department of Hepatobiliary Intervention, Beijing Tsinghua Changgung Hospital, School of Clinical Medicine, Tsinghua University, Beijing, China; [3]Department of Chemistry, Durham University, Stockton Road, Durham DH1 3LE, U.K.; [4]Key Laboratory of Carcinogenesis and Translational Research (Ministry of Education), Center Laboratory, Peking University Cancer Hospital & Institute, Beijing, China

Abstract: Tumor samples of pancreatic ductal adenocarcinoma patients, who underwent resection surgery, were implanted into NOD/SCID mice to construct pancreatic cancer patient-derived xenograft (PDX) models and explore the biological changes in the different generations of PDXs. Ten PDXs were successfully generated, and the tumor formation rate of F1 PDXs was found to be 38.46%, which was lower than F2 (77.78%) and F3 (71.43%) PDXs. In addition, latent periods of tumorigenesis of F2 and F3 PDXs were significantly shorter, compared to that in F1 PDXs ($P<0.05$). Comparison of H&E staining of tumor tissue from primary pancreatic cancer and PDXs showed that all three generations of PDXs had similar histopathology to primary pancreatic cancer, indicating that PDXs may well reproduce the histological patterns of primary human cancer. Besides, Ki67 expression was increased in all three generations of PDXs compared to primary tumors of patients, and additionally, EpCAM expression was increased in F3 PDXs. These results were corroborated by the real-time qPCR and western blot results. Therefore, we concluded that PDXs are able to preserve the differentiation degree, morphological characteristics, and structural features of tumor cells. Furthermore, the latent periods of tumorigenesis are shortened after the first generation, which may be attributed to an increase in expression levels of tumor promoters such as Ki67 and EpCAM. PDX models may become an efficient tool for pancreatic cancer research.

Keywords: Pancreatic cancer, patient-derived xenograft, animal model

Introduction

Pancreatic ductal adenocarcinoma (PDAC) is currently the 4th leading cause of cancer death, with an overall 5-year survival rate of approximately 5% [1, 2]. Most patients with PDAC, have advanced disease at the time of diagnosis and have lost the opportunity of resection surgery for the lack of visible and distinctive symptoms and reliable biomarkers for early diagnosis. Only around 15% of patients undergo resection, while for the remaining 85% of patients, chemotherapy and radiation are the only treatment options [3, 4]. The lack of effective anti-cancer drugs is one of the main reasons for the low treatment effective rate and survival rate of pancreatic cancer. However, research on anti-cancer drugs rely on suitable animal models. Currently, the animal models used for drug evaluation are generally the xenograft models derived from human tumor cell lines which have been cultured in vitro [5, 6]. Although these models do have application value in evaluating drug toxicity and prognosis, the efficiency of drugs cannot be accurately judged due to genetic variations and the absence of tumor microenvironment. Therefore, it is necessary to construct an animal model that can more accurately reflect the development of human tumor, in order to overcome these problems [6-8].

Patient-derived xenograft (PDX) models have become popular in recent years; PDX models are established by subcutaneously transplanting tumor tissues of patients into immunodeficient mice, such as NOD/SCID (Non-obese diabetic/severe combined immunodeficiency) mice, which can mimic the tumor microenvironment as primary tumors in the human body [9-12]. PDXs from various tumors have been constructed, such as breast cancer [13], colorectal cancer [14], and renal cell carcinoma [15]. However, due to low success rate, long tumorigenesis period, and high cost, the use of PDXs in clinical trials is still limited. Therefore, our responsibility in the long research path will be to resolve these problems and improve the success rate of PDX generation. In this study, we focus on the differences between the generations of PDXs, arising during PDX line passaging, and oncological factors affecting tumor formation rate.

Materials and methods

Patients and samples

Surgically resected tumor specimens (n=31) and paired adjacent normal pancreatic tissues were obtained from patients diagnosed with pancreatic carcinomas, who underwent surgery at the Peking University Cancer Hospital from November 2013 to January 2014. None of these patients received chemotherapy or radiation therapy before surgery. Each specimen obtained, measured approximately 1×1×1 cm in size. Fresh tumor specimens were divided into three parts: one part was transferred to antibiotic-containing Dulbecco's modified Eagle's medium (DMEM; GibcoBRL, Life Technologies, Grand Island, NY, USA) for tumor transplantation; one part was fixed in 4% formalin for Hematoxylin-eosin (H&E) or immunohistochemistry (IHC) staining; and the rest was immediately transferred to liquid nitrogen and stored at -80°C for future studies. Each part measured approximately 5×5×5 mm. This study was approved by the medical ethics committee of Peking University Cancer Hospital and was carried out in accordance with the approved guidelines.

Establishment of PDX models

All tumor specimens from the patients (termed F0) were subcutaneously inoculated into the right buttock of 5-week-old female NOD/SCID mice (Beijing HFK Bio-Technology Co., LTD, Beijing, China), weighting 18-20 g. Tumor specimens were cut into small pieces (less than 1 mm^3) and mixed with Matrigel (100 μl per sample) (BD Biosciences, Heidelberg, Germany) for 20 seconds at room temperature, immediately prior to xenotransplantation. Tumor growth was measured twice a week by a Vernier caliper, using the following formula: tumor volume = [length × width^2]/2 as previously reported [16]. When the tumor size reached approximately 1000 mm^3, the xenograft mouse was sacrificed under anesthesia, and the tumor was excised and divided into three parts, identical to the procedure followed for the human specimens. The DMEM-stored portion was used to re-inoculate the mice to obtain subsequent generations containing the tumor mass. This generation of mice, receiving the patient tumor transplant, was termed F1. Similarly, the following generations were termed F2, F3...Fn respectively [17]. Therefore, PDXs derived from one patient was called a PDX line. Mice were kept in the animal facilities of the Peking University Cancer Hospital and maintained in specified pathogen-free conditions. Animals were exposed to 12 h light/12 h darkness cycles and provided with standard food and water *ad libitum*. All procedures were performed under sterile conditions and carried out in accordance with the Guide for the Care and Use of Laboratory Animals of the National Institutes of Health.

RNA extraction and gene expression analysis

RNA was extracted from the tumor and adjacent normal tissue of patients, and from the xenograft tissue of the PDXs, using TRIZOL reagent (Thermo Fisher Scientific), according to the manufacturer's instructions. cDNA was synthesized from the extracted RNA, using the EasyScript First-Strand cDNA Synthesis SuperMix kit (Invitrogen). PCR amplification was performed using the following primers: EpCAM, 5'-GCAGCTGTGGGTTGATTCCA-3' (forward) and 5'-GGGCCAGACCATCGCTATCT-3' (reverse); MKI67, 5'-CCTTTGGTGGGCACCTAAGA-3' (forward) and 5'-CTTTTGGTTGGGGCTTCTCC-3' (reverse); KRAS, 5'-TGCCTTGACGATACAGCTAA-3' (forward) and 5'-CCAAGAGACAGGTTTCTCCA-3' (reverse); GAPDH, 5'-AAGACGGGCGGAGAGAAACC-3' (forward) and 5'-CGACCAAATCCGTTGACTC-CG-3' (reverse). Quantitative detection of the relative mRNA levels for the EpCAM, MKI67,

and KRAS genes was performed with ABI 7500 Fast Real-Time PCR System. PCR amplification was carried out in a total volume of 20 µl, containing 1 µl cDNA solution, 10 µl of 2×qPCR MasterMix (ABM, Inc.), 1 µl each primer at 5 µM concentration, and 7 µL of nuclease-free water. GAPDH was quantified and used for the normalization of expression values of the other genes. The $2^{-\Delta\Delta CT}$ method of relative quantification was used to determine the fold change in expression. Here, the threshold cycle (C_T) values of the target mRNAs were first normalized to the C_T values of the internal control, GAPDH, in the same samples ($\Delta C_T = C_{Ttarget} - C_{TGAPDH}$), and further normalized with the internal control (adjacent normal tissues of patients were used as internal control) ($\Delta\Delta C_T = \Delta C_T - \Delta C_{Tcon}$). Fold change in expression was then obtained ($2^{-\Delta\Delta C_T}$).

Western blot analysis

About 50 mg of tissue was homogenized in T-PER™ Tissue Protein Extraction Reagent (Thermo Scientific, Inc.). Protein concentration was determined using the Bradford method. About 30 µg of protein was subjected to sodium dodecyl sulfate polyacrylamide gel electrophoresis (SDS-PAGE) on 10% polyacrylamide gels. Thereafter, proteins were electrophoretically transferred to polyvinylidene fluoride (PVDF) membranes (Millipore, Bedford, MA, USA). After transferring, the membranes were blocked for 2 h at room temperature with 5% nonfat dry milk in TBS-Tween 20 (TBS-T), followed by incubation overnight at 4°C with the following primary antibodies: anti-EpCAM antibody (1:1000, Abcam, Cambridge, MA, USA, cat # ab71916), anti-KRAS antibody (1:500, Abcam, Cambridge, MA, USA, cat # ab180772) and anti-β-actin antibody (1:1000, CST, Danvers, MA, USA, cat # 4967). After three washes in TBS-T, membranes were probed with the appropriate HRP-linked secondary antibodies. The blots were visualized by luminal chemiluminescence ChemiDoc XRS (Bio-Rad) and scanned by Quantity One v 4.6.2 software (Bio-Rad). The protein band density was measured using Quantity One v 4.6.2 software (Bio-Rad).

H&E and immunohistochemistry staining

Patient tumor specimens or xenografts were fixed in 4% formalin solution before embedding. H&E staining kits (C0105, Beyotime, China) were used to perform H&E staining following the manufacturer's instruction. IHC experiments were performed as described previously [18]. States of Ki67 and EpCAM (Epithelial Cell Adhesion Molecule) expression were evaluated using anti-Ki67 (1:100; ab15580, Abcam Inc., Cambridge, CA, USA) and anti-EpCAM (1:10000; ab71916, Abcam Inc., Cambridge, MA) antibodies in every tumor specimen obtained from patient or PDX. H&E and IHC staining was reviewed and scored by two independent pathologists who were blinded to this study. For the semiquantitative evaluation of Ki67 and EpCAM staining, the Remmele/Stegner immunoreactive score (IRS score) [19] was used. The intensity of cytoplasmic expression was graded from 0 to 3: 0 as negative staining; 1 as weak; 2 as medium; 3 as strong intensity. The score was obtained by multiplying the grade with a factor determined by the percentage of positive tumor cells (0-10%/1; 10-50%/2; 50-80%/3; 80-100%/4).

Statistical analysis

Unpaired 2-tailed *t* tests were used for group comparisons after verifying normality and homogeneity of variance. Differences in the tumor volumes and comparison of gene expression for these groups were analyzed using one-way analysis of variance (ANOVA). The relationships between clinicopathological characteristics and transplantation rate of xenografts were analyzed using the chi-square test and Fisher's exact test. All 26 pancreatic cancer patients were evaluated for overall survival (OS) and progression-free survival (PFS). OS was defined as the elapsed time between the inclusion date and death due to any cause. PFS was defined as the elapsed time between the date of inclusion and the date of tumor progression. All 26 patients did not die within 30 days of surgery. The Kaplan-Meier method was used to analyze OS or PFS, and log-rank test was used to estimate the difference. *P* values less than 0.05 (*P*<0.05) were considered to be statistically significant. All statistical analyses were performed using IBM SPSS 25.0 software (SPSS Inc., Chicago, IL, USA).

Results

Clinicopathological characteristics of the patients

Fresh pancreatic tumor tissues were obtained from 31 patients totally to establish the PDX

Figure 1. Flow diagram from acquisition of pancreatic tumor to transplantation in mice.

was performed to compare the histopathology between patient tumors and xenograft tumors. Our results showed that PDXs could preserve tumor glandular structure of pancreatic ductal adenocarcinoma, degree of differentiation, and stromal content (**Figure 2**; **Table 3**).

Comparison of relevant biomarkers

We compared the mRNA expression of MKI67, EpCAM and KRAS in patient tumors and xenograft tumors by qPCR (**Figure 3A-C**, respectively). The results showed that, mRNA expression of MKI67, EpCAM and KRAS was increased in all generations of PDXs as compared to that in the tumors from patients (F0). Furthermore, significant differences were observed in MKI67 expression of F1 PDXs compared to F0 (*P*= 0.040) and in EpCAM expression of both F2 and F3 PDXs, compared to F0 (*P*=0.031, *P*=0.020, respectively). Western blot results further verified the increased expression of EpCAM and KRAS in the three generations of PDXs, compared to F0 (**Figure 3D**). We further reconfirmed the Ki67 and EpCAM expression in patient tumors and xenograft tumors by IHC (**Figure 3E**, **3F**, respectively). Indeed, mean IRS for Ki67 in F1 (9.8±2.0), F2 (10.6±1.9), and F3 (10.6±1.9) were significantly higher than in the primary patient tumors (F0) (7±1.41) (*P*=0.03, *P*=0.007, *P*=0.007, respectively) (**Figure 3G**). However, mean IRS for EpCAM, was significantly higher only in F3 (11.4±1.3), compared to F0 (7.8±2.7) (*P*=0.016) (**Figure 3H**).

Correlation between transplantation rate of F1 PDXs and clinicopathological characteristics

Our results showed that the transplantation rate of F1 PDXs displayed statistically significant association with alcohol consumption (P=0.049) (**Table 4**). However, no significant correlations between transplantation rate of F1 PDXs and other clinicopathological characteristics was observed.

Correlation of transplantation rate of F1 PDXs with postoperative survival

The survival analysis results demonstrated no statistically significant association between transplantation rate of F1 PDXs and OS or PFS (**Figure 4**). Therefore, the transplantation rate of F1 PDXs may not be a predictor of prognosis in these patients.

models. Among these cases, 5 patients were diagnosed with non-ductal adenocarcinoma and were excluded. The other 26 patients were finally enrolled for the xenograft study (**Figure 1**). The details of these enrolled patients are listed in **Table 1**. The average age of the patients was 60.38 years (60.38±11.2); females and males comprised 53.8% (n=14) and 46.2% (n=12), respectively. Majority of these tumors occurred in the body and tail of the pancreas, most of them showing middle differentiation. Lymph node (LN) metastasis was present in 46.2% of the patients (n=12), while one patient was diagnosed with distant metastasis.

PDX generation in NOD/SCID mice

We successfully produced 10 F1 PDXs out of the 26 tumor grafted, representing a 38.46% success rate. The observed success rate of the following F2 and F3 PDXs were 77.78% and 71.43%, respectively. Success rates of F2 and F3 were higher than F1 PDXs (**Table 2**), although the difference was not statistically significant. Furthermore, the average time to tumor formation of F2 and F3 PDXs were 56.43±12.37 and 51.20±11.34 days, respectively, both being significantly higher than that of the F1 PDXs (71.50±28.44). Furthermore, the F3 PDXs showed a significantly shorter time for tumor formation than the F2 PDXs.

Comparison of histopathological characteristics

Differentiation of xenografts was judged and compared to the primary tumors of patients by two independent pathologists. H&E staining

Table 1. Clinicopathological features of the 26 pancreatic cancer patients

Clinicopathological features	No. of patients	% of patients
Gender		
Female	14	53.8
Male	12	46.2
Age (years)		
<60	12	46.2
≥60	14	53.8
Smoking history		
No	19	73.1
Yes	7	26.9
History of alcohol consumption		
No	21	80.8
Yes	5	19.2
Tumor size (cm)		
<3.8	13	50.0
≥3.8	13	50.0
Tumor location		
Head	8	30.8
Body/tail	18	69.2
Vascular thrombosis		
No	15	57.7
Yes	11	42.3
Differentiation		
Moderate	20	76.9
Poor	6	23.1
TNM stage		
I-II	12	46.2
III-IV	14	53.8
Lymph node metastasis		
Present	12	46.2
Absent	14	53.8
Distant metastasis		
Present	1	3.8
Absent	25	96.2
CA19-9 (U/ml)		
<1400	19	73.1
≥1400	7	26.9
CEA (ng/ml)		
<17	22	84.6
≥17	4	15.4
CA72-4 (U/ml)		
<8	18	69.2
≥8	8	30.8
CA242 (U/ml)		
<90	19	73.1
≥90	7	26.9

Discussion

Pancreatic cancer has become the fourth leading cause of cancer-related death worldwide, and the overall 5-year survival rate is less than 5% [20]. Surgery remains the only option to cure pancreatic cancer, and raises the 5-year survival rate up to approximately 20% [21]. However, most patients miss the opportunity of surgical resection when diagnosed with pancreatic cancer, therefore chemotherapy becomes one of the main options for treatment. Both palliative chemotherapy and adjuvant chemotherapy can prolong the survival time of patients to some extent, while due to individual differences, the overall effect is limited. To predict the effect of anti-cancer agents before administering to patients, animal models are enrolled in most of the drug pre-clinical studies. Currently, most of the pancreatic cancer animal models are generated by inoculating human cell lines into immunodeficient animals. Although, these models are useful for quantifying the growth of tumor cells in vivo, they often do not maintain the proliferation pattern and structures of the original tumors. Furthermore, due to prolonged culture in vitro, the information about tumor microenvironment might be lost. Therefore, animal models based on cell line inoculation cannot reflect the condition of the original tumor objectively. Therefore, animal models possessing the characteristic of patient tumors are urgently needed in cancer research.

The use of patient-derived xenografts provides convincing experimental evidence to the development of personalized medicine. Besides, PDXs have been used to evaluate the effects of anti-cancer drug combinations, identify biomarkers and help studies of resistance mechanisms [22]. Generally, most researchers choose NOD/SCID mice to generate PDXs, which are produced by hybridizing severe combined immunodeficiency (SCID) mice, lacking functional B and T cells, and non-obese diabetic (NOD) mice [23]. The NOD/SCID mice have additional immunological defects, including low natural killer (NK) cell function and absence of circulating complement components [24]. The success rate of xenotransplantation in NOD/SCID mice was significantly higher than that of SCID mice, making the NOD/SCID mice an ideal animal for the study of PDXs. However, studies evaluating the differences among passages of PDXs are

Table 2. Tumor formation rate and latency period of xenografts

	F1 mice	F2 mice	F3 mice
Tumor formation rate (success/total PDX lines)	38.46% (10/26)	77.78% (7/9)	71.43% (5/7)
Mean time (days)	71.50±28.44	56.43±12.37[*]	51.20±11.34[*,#]
Metastasis	-	-	-

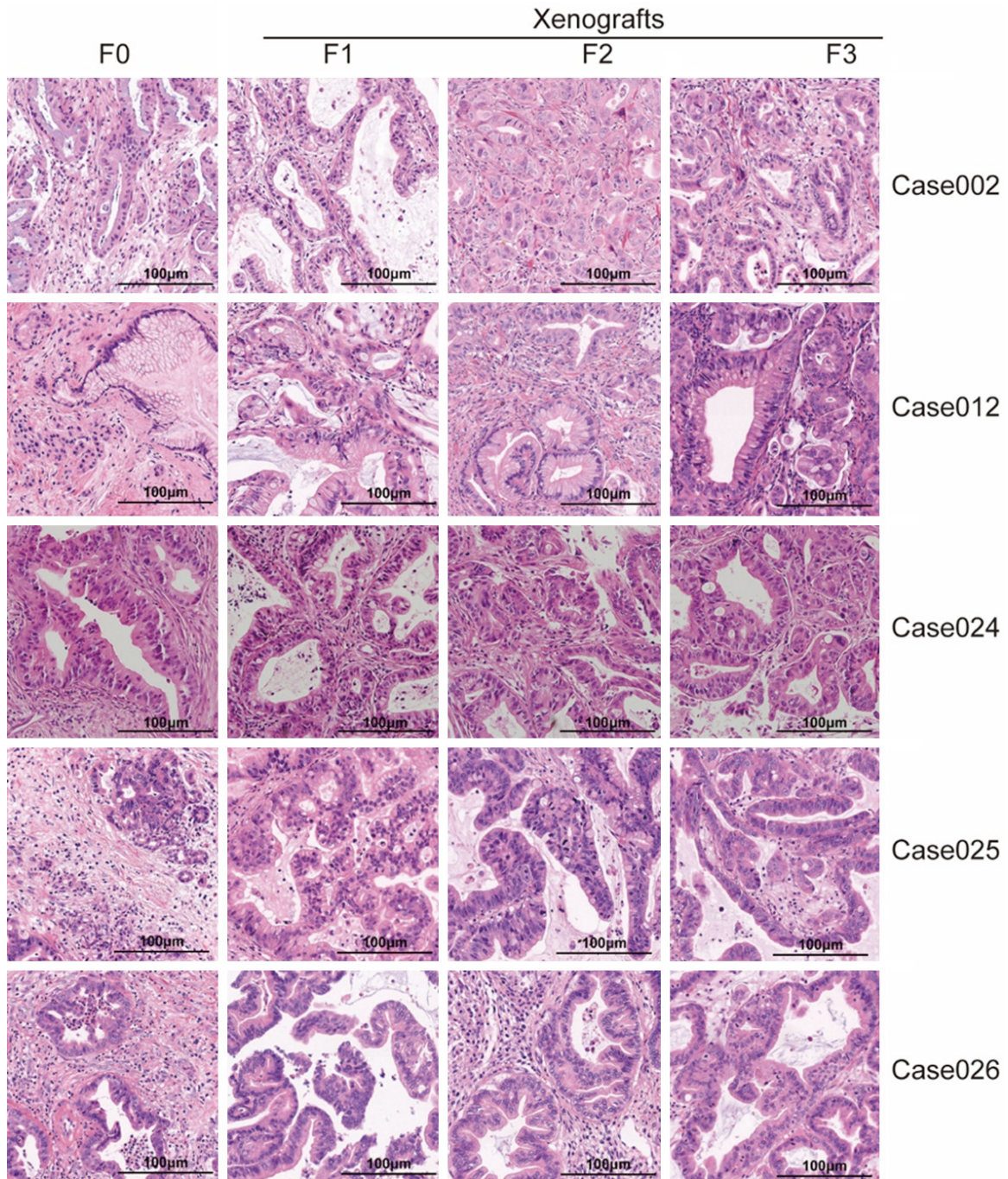[*]Compared with F1 PDXs, $P<0.01$. [#]Compared with F2 PDXs, $P<0.01$.

Figure 2. PDX generation in NOD/SCID mice. Representative H&E staining results of tumors from five patients and their three corresponding passages of xenografts (×200).

Table 3. Comparison of differentiation of primary tumors of patients and xenografts

Case	Patient primary tumor	Xenograft		
		F1	F2	F3
002	Moderate	Moderate	Moderate	Moderate
012	Moderate	Moderate	Moderate	Moderate
024	Moderate	Moderate	Moderate	Moderate
025	Moderate	Moderate	Moderate	Moderate
026	Moderate	Moderate	Moderate	Moderate

rare. DeRose Y.S. *et al.* found that after several generations of transplantation, mesenchymal cells from the original tumor of the patient were gradually replaced by the mesenchymal cells of mice that caused the enrichment of cytokeratin expression in the tissues [11]. Therefore, it is necessary to further study how the characteristic of original tumor changes during PDX line passaging.

Previous studies have reported the tumor formation rate of PDXs to be around 40%-60% [25-29]. In our study, the tumor formation rate of F1 PDXs was slightly lower than that reported in previous studies, which may be attributed to the following reasons: 1. Degree of differentiation of the tumors in the enrolled patients were varied in different reports, success rates of xenografts tend to be higher with tumors resected from highly malignant pancreatic cancers; 2. Only 26 cases of pancreatic duct adenocarcinoma patients were observed in our study, therefore limitations associated with small sample size may have been responsible for the observed discrepancy; 3. Restricted by surgical specimens, each original tumor was transplanted into one NOD/SCID mouse, therefore, individual differences between mice might have affected the results. According to a previous study, it takes 1-12 months to develop tumors in the first generation of PDXs, after which, the time for tumor generation is reduced in the following generations, usually being 1-6 months for the F2 PDXs [30]. Uncertain tumor cell content, presence of necrotic tissue or macrophages and NK cells in the fresh tumor specimens resected from patients, may lead to a lower tumor formation rate in the F1 PDXs. Furthermore, samples with low tumorigenicity might have been selected for establishment of the F1 PDXs, leading to longer latent periods of tumorigenesis. Nonetheless, tumor formation

rates of the F2 and F3 PDXs were greatly improved, and the latent periods of tumorigenesis were shorter than the F1 PDXs. As the latent periods of tumorigenesis of the F3 PDXs were slightly shorter than that of the F2 PDXs, we reckon that the malignancy and microenvironment were more stable after expanding the PDX lines. Comparison of the tumor formation rates in all three generations of PDX lines displayed no statistical significance, which may be attributed to the small sample size.

H&E staining results of primary and PDX tumors showed that PDXs could reproduce the histological morphology and pathology, as well as the degree of differentiation of the original tumors. Moreover, the characteristics of the cellular structure were maintained during passages (**Figure 2**; **Table 3**). The gene expression levels of MKI67 and EpCAM were increased in PDXs during passaging of the tumor (**Figure 3A**, **3B**). KRAS gene expression also showed an increase, although it was not statistically significant (**Figure 3C**). The protein expression results of EpCAM and KRAS also corroborated the findings of the gene expression experiments (**Figure 3D**). Furthermore, the results of IHC for Ki67 and EpCAM showed that, during passage of the tumor in the PDXs, Ki67 expression was significantly increased in all three generations of PDXs, while EpCAM expression was significantly increased only in the third generation (**Figure 3**). As it is widely known, Ki67 is usually used as a proliferative marker [31, 32], and can specifically label proliferative cells at mitotic phase [33]. EpCAM is a transmembrane glycoprotein involved in cell-cell interactions and cell-stroma adhesion [34]. EpCAM is highly up-regulated in virtually all epithelial carcinomas, including pancreatic cancers [35-38]. Since there are no specific biomarkers for pancreatic cancer, we chose Ki67 and EpCAM to determine whether PDX lines could duplicate the malignancy and expression pattern of some of the biomarkers of the primary tumor. Indeed, our results showed that PDX lines not only maintained the expression of Ki67 and EpCAM, but in addition, the expression level of these markers was increased. These interesting findings may explain the shorter latent periods of F2 and F3 PDXs, compared to the F1 PDXs, to some extent. KRAS is one of the most frequently mutated proto-oncogenes in PDAC patients, and besides mutations, overexpression, allelic
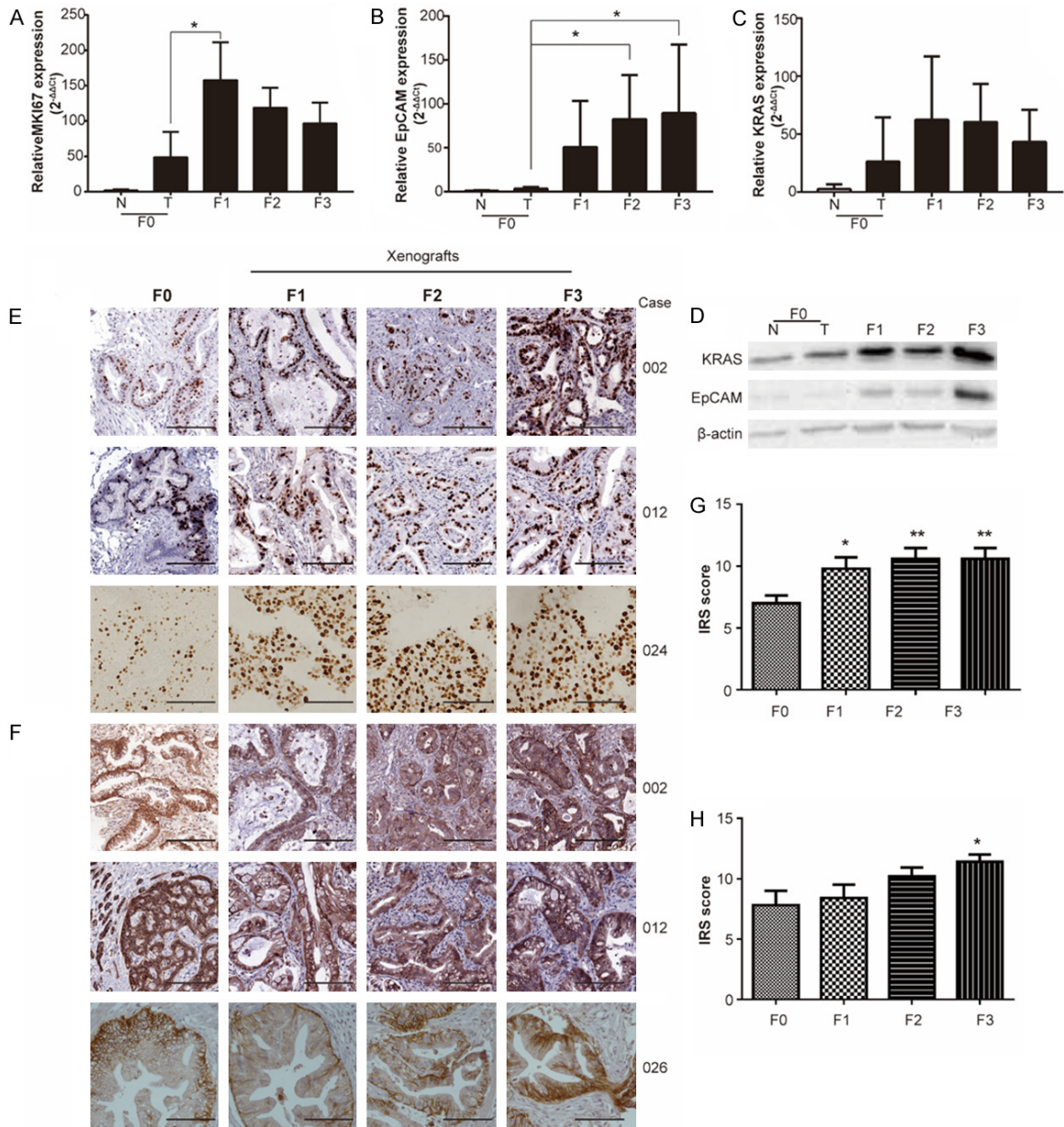
Figure 3. Expression of relative biomarker. A. qPCR result of MKI67 gene expression; B. qPCR result of EpCAM gene expression; C. qPCR result of KRAS gene expression; D. Western blot result of KRAS and EpCAM; E. Representative IHC results of Ki67 expression of F0 and three corresponding passages of xenografts; F. Representative IHC results of EpCAM expression of F0 and three corresponding passages of xenografts; G. Immunoreactive Remmele-Stegner Score (IRS) for Ki67 expression. H. IRS for EpCAM expression. *$P<0.05$, **$P<0.01$ compared with tumors of F0. (×200, bar in the lower right corner of each photo represents 100 μm).

imbalance, and gene fusion are also known to activate KRAS [39]; activated KRAS can transform normal cells into malignant cells [40, 41]. In our research, KRAS gene and protein level showed an increasing trend during tumor passage in PDXs, although it was not statistically significant. This may be attributed to the limited number of samples in our study.

To our surprise, the transplantation rate of F1 PDXs was found to be significantly correlated to alcohol consumption (**Table 4**). Yuri Persidsky et al. have reported that alcohol abuse had influence on neuroinflammation and impaired immune responses in animal models based on NOD/SCID mice [42]. While there are no reports on whether the alcohol level in patients' blood

Table 4. Correlations between transplantation rate and clinicopathological parameters

Clinicopathological features	No. of patients (%)	Transplantation rate (%)	P
Gender			0.483
Female	14 (53.8%)	50.0% (7/14)	
Male	12 (46.2%)	25.0% (3/12)	
Age (years)			0.191
<60	12 (46.2%)	25.0% (3/12)	
≥60	14 (53.8%)	50.0% (7/14)	
Smoking history			0.124
No	19 (73.1%)	47.4% (9/19)	
Yes	7 (26.9%)	14.3% (1/7)	
History of alcohol consumption			0.049
No	21 (80.8%)	47.6% (10/21)	
Yes	5 (19.2%)	0.0% (0/5)	
Tumor size (cm)			0.420
<3.8	13 (50.0%)	30.8% (4/13)	
≥3.8	13 (50.0%)	46.2% (6/13)	
Tumor location			0.420
Head	8 (30.8%)	50.0% (4/8)	
Body/tail	18 (69.2%)	33.3% (6/18)	
Vascular thrombosis			0.315
No	15 (57.7%)	46.7% (7/15)	
Yes	11 (42.3%)	27.3% (3/11)	
Nerve invasion			0.192
No	9 (34.6%)	55.6% (5/9)	
Yes	17 (65.4%)	29.4% (5/17)	
Differentiation			0.508
Moderate	20 (76.9%)	35.0% (7/20)	
Poor	6 (23.1%)	50.0% (3/6)	
TNM stage			0.756
I-II	12 (46.2%)	41.7% (5/12)	
III-IV	14 (53.8%)	35.7% (5/14)	
Lymph node metastasis			0.619
Present	12 (46.2%)	33.3% (4/12)	
Absent	14 (53.8%)	42.9% (6/14)	
Distant metastasis			0.529
Present	1 (3.8%)	0.0% (0/1)	
Absent	25 (96.2%)	40.0% (10/25)	
CA19-9 (U/ml)			0.780
<1400	19 (73.1%)	36.8% (7/19)	
≥1400	7 (26.9%)	42.9% (3/7)	
CEA (ng/ml)			0.102
<17	22 (84.6%)	31.9% (7/22)	
≥17	4 (15.4%)	75.0% (3/4)	
CA72-4 (U/ml)			0.946
<8	18 (69.2%)	38.9% (7/18)	
≥8	8 (30.8%)	37.5% (3/8)	
CA242 (U/ml)			0.235
<90	19 (73.1%)	31.6% (6/19)	
≥90	7 (26.9%)	57.1% (4/7)	

has specific effects on mice, we shall enroll more patients in our further study to validate the findings and reveal the potential molecular mechanisms.

PDXs have strong application value for testing new anti-cancer drugs and drug combinations in pancreatic cancer research. However, due to low success rate, long tumorigenesis period and high cost, the use of PDXs in clinical trials is restricted. In our future research, we will focus on how to improve the tumor formation rate and shorten the tumorigenesis period. The first three generations of PDXs are particularly important, as after F3 PDXs, we can expand passage and start drug sensitivity tests. Usually, the first three generations of PDXs are used to breed conservation. Therefore, data from only the first three generations of PDXs were collected in our study, and we will continue to further study the tumorigenesis mechanism of PDXs and carry out drug susceptibility experiments in the future to get more in-depth and comprehensive data. We hope that our research will provide a comprehensive and objective basis for PDX study.
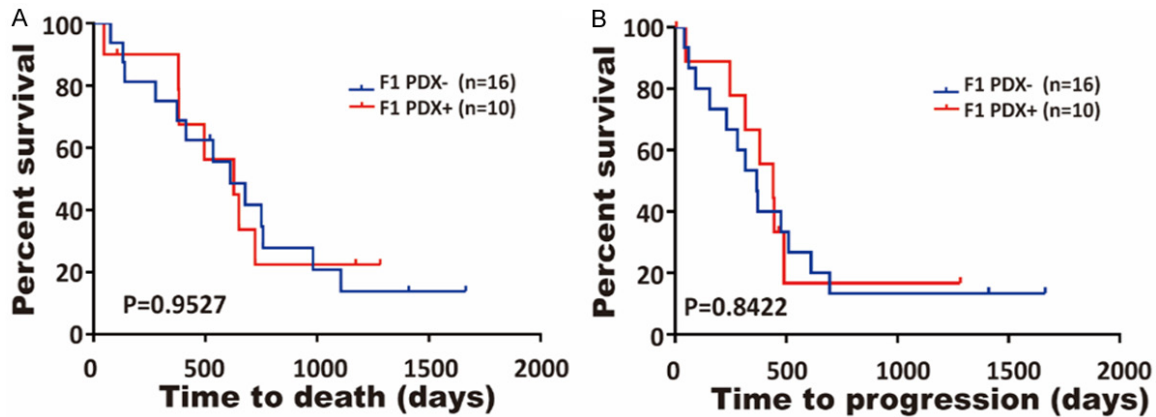
Acknowledgements

Figure 4. Correlation of tumor formation rate of F1 PDXs with postoperative overall survival (A) and progression-free survival (B) of pancreatic cancer patients.

Informed consent was obtained from all individual participants included in the study.

Disclosure of conflict of interest

None.

Address correspondence to: Chun-Yi Hao, Key Laboratory of Carcinogenesis and Translational Research (Ministry of Education), Department of Hepato-Pancreato-Biliary Surgery, Peking University Cancer Hospital & Institute, CRBII Room 342, No. 52 Fucheng Road, Haidian District, Beijing 100142, China. Tel: +86-10-88196182; Fax: +86-10-8819-6548; E-mail: haochunyi@bjmu.edu.cn

References

[1] Siegel R, Ma J, Zou Z and Jemal A. Cancer statistics, 2014. CA Cancer J Clin 2014; 64: 9-29.

[2] Ryan DP, Hong TS and Bardeesy N. Pancreatic adenocarcinoma. N Engl J Med 2014; 371: 2140-2141.

[3] Vincent A, Herman J, Schulick R, Hruban RH and Goggins M. Pancreatic cancer. Lancet 2011; 378: 607-620.

[4] Mian OY, Ram AN, Tuli R and Herman JM. Management options in locally advanced pancreatic cancer. Curr Oncol Rep 2014; 16: 388.

[5] Morton CL and Houghton PJ. Establishment of human tumor xenografts in immunodeficient mice. Nat Protoc 2007; 2: 247-250.

[6] Sausville EA and Burger AM. Contributions of human tumor xenografts to anticancer drug development. Cancer Res 2006; 66: 3351-3354, discussion 3354.

[7] Hidalgo M, Amant F, Biankin AV, Budinska E, Byrne AT, Caldas C, Clarke RB, de Jong S, Jonkers J, Maelandsmo GM, Roman-Roman S, Seoane J, Trusolino L and Villanueva A. Patient-derived xenograft models: an emerging platform for translational cancer research. Cancer Discov 2014; 4: 998-1013.

[8] Gillet JP, Varma S and Gottesman MM. The clinical relevance of cancer cell lines. J Natl Cancer Inst 2013; 105: 452-458.

[9] Wang Y, Revelo MP, Sudilovsky D, Cao M, Chen WG, Goetz L, Xue H, Sadar M, Shappell SB, Cunha GR and Hayward SW. Development and characterization of efficient xenograft models for benign and malignant human prostate tissue. Prostate 2005; 64: 149-159.

[10] Dong X, Guan J, English JC, Flint J, Yee J, Evans K, Murray N, Macaulay C, Ng RT, Gout PW, Lam WL, Laskin J, Ling V, Lam S and Wang Y. Patient-derived first generation xenografts of non-small cell lung cancers: promising tools for predicting drug responses for personalized chemotherapy. Clin Cancer Res 2010; 16: 1442-1451.

[11] DeRose YS, Wang G, Lin YC, Bernard PS, Buys SS, Ebbert MT, Factor R, Matsen C, Milash BA, Nelson E, Neumayer L, Randall RL, Stijleman IJ, Welm BE and Welm AL. Tumor grafts derived from women with breast cancer authentically reflect tumor pathology, growth, metastasis and disease outcomes. Nat Med 2011; 17: 1514-1520.

[12] Bock BC, Stein U, Schmitt CA and Augustin HG. Mouse models of human cancer. Cancer Res 2014; 74: 4671-4675.

[13] Marangoni E, Vincent-Salomon A, Auger N, Degeorges A, Assayag F, de Cremoux P, de Plater L, Guyader C, De Pinieux G, Judde JG, Rebucci M, Tran-Perennou C, Sastre-Garau X, Sigal-Zafrani B, Delattre O, Dieras V and Poupon MF. A new model of patient tumor-derived breast cancer xenografts for preclinical assays. Clin Cancer Res 2007; 13: 3989-3998.

[14] Linnebacher M, Maletzki C, Ostwald C, Klier U, Krohn M, Klar E and Prall F. Cryopreservation of human colorectal carcinomas prior to xenografting. BMC Cancer 2010; 10: 362.

[15] Sivanand S, Pena-Llopis S, Zhao H, Kucejova B, Spence P, Pavia-Jimenez A, Yamasaki T, McBride DJ, Gillen J, Wolff NC, Morlock L, Lotan Y, Raj GV, Sagalowsky A, Margulis V, Cadeddu JA, Ross MT, Bentley DR, Kabbani W, Xie XJ, Kapur P, Williams NS and Brugarolas J. A validated tumorgraft model reveals activity of dovitinib against renal cell carcinoma. Sci Transl Med 2012; 4: 137ra175.

[16] Rubio-Viqueira B, Jimeno A, Cusatis G, Zhang X, Iacobuzio-Donahue C, Karikari C, Shi C, Danenberg K, Danenberg PV, Kuramochi H, Tanaka K, Singh S, Salimi-Moosavi H, Bouraoud N, Amador ML, Altiok S, Kulesza P, Yeo C, Messersmith W, Eshleman J, Hruban RH, Maitra A and Hidalgo M. An in vivo platform for translational drug development in pancreatic cancer. Clin Cancer Res 2006; 12: 4652-4661.

[17] Stebbing J, Paz K, Schwartz GK, Wexler LH, Maki R, Pollock RE, Morris R, Cohen R, Shankar A, Blackman G, Harding V, Vasquez D, Krell J, Zacharoulis S, Ciznadija D, Katz A and Sidransky D. Patient-derived xenografts for individualized care in advanced sarcoma. Cancer 2014; 120: 2006-2015.

[18] Zhang Y, Tian X, Ji H, Guan X, Xu W, Dong B, Zhao M, Wei M, Ye C, Sun Y, Yuan X, Yang C and Hao C. Expression of SATB1 promotes the growth and metastasis of colorectal cancer. PLoS One 2014; 9: e100413.

[19] Thaiss WM, Kaufmann S, Kloth C, Nikolaou K, Bosmuller H and Horger M. VEGFR-2 expression in HCC, dysplastic and regenerative liver nodules, and correlation with pre-biopsy Dynamic Contrast Enhanced CT. Eur J Radiol 2016; 85: 2036-2041.

[20] Gong Z, Holly EA and Bracci PM. Survival in population-based pancreatic cancer patients: San Francisco Bay area, 1995-1999. Am J Epidemiol 2011; 174: 1373-1381.

[21] Hackert T, Buchler MW and Werner J. Surgical options in the management of pancreatic cancer. Minerva Chir 2009; 64: 465-476.

[22] Malaney P, Nicosia SV and Dave V. One mouse, one patient paradigm: new avatars of personalized cancer therapy. Cancer Lett 2014; 344: 1-12.

[23] Shultz LD, Schweitzer PA, Christianson SW, Gott B, Schweitzer IB, Tennent B, McKenna S, Mobraaten L, Rajan TV and Greiner DL. Multiple defects in innate and adaptive immunologic function in NOD/LtSz-scid mice. J Immunol 1995; 154: 180-191.

[24] Lock RB, Liem N, Farnsworth ML, Milross CG, Xue C, Tajbakhsh M, Haber M, Norris MD, Marshall GM and Rice AM. The nonobese diabetic/severe combined immunodeficient (NOD/SCID) mouse model of childhood acute lymphoblastic leukemia reveals intrinsic differences in biologic characteristics at diagnosis and relapse. Blood 2002; 99: 4100-4108.

[25] Jun E, Jung J, Jeong SY, Choi EK, Kim MB, Lee JS, Hong SM, Seol HS, Hwang C, Hoffman RM, Shim IK, Chang S and Kim SC. Surgical and oncological factors affecting the successful engraftment of patient-derived xenografts in pancreatic ductal adenocarcinoma. Anticancer Res 2016; 36: 517-521.

[26] Thomas RM, Truty MJ, Kim M, Kang Y, Zhang R, Chatterjee D, Katz MH and Fleming JB. The canary in the coal mine: the growth of patient-derived tumorgrafts in mice predicts clinical recurrence after surgical resection of pancreatic ductal adenocarcinoma. Ann Surg Oncol 2015; 22: 1884-1892.

[27] Garcia PL, Miller AL, Kreitzburg KM, Council LN, Gamblin TL, Christein JD, Heslin MJ, Arnoletti JP, Richardson JH, Chen D, Hanna CA, Cramer SL, Yang ES, Qi J, Bradner JE and Yoon KJ. The BET bromodomain inhibitor JQ1 suppresses growth of pancreatic ductal adenocarcinoma in patient-derived xenograft models. Oncogene 2016; 35: 833-845.

[28] Garrido-Laguna I, Uson M, Rajeshkumar NV, Tan AC, de Oliveira E, Karikari C, Villaroel MC, Salomon A, Taylor G, Sharma R, Hruban RH, Maitra A, Laheru D, Rubio-Viqueira B, Jimeno A and Hidalgo M. Tumor engraftment in nude mice and enrichment in stroma- related gene pathways predict poor survival and resistance to gemcitabine in patients with pancreatic cancer. Clin Cancer Res 2011; 17: 5793-5800.

[29] Jin K, Teng L, Shen Y, He K, Xu Z and Li G. Patient-derived human tumour tissue xenografts in immunodeficient mice: a systematic review. Clin Transl Oncol 2010; 12: 473-480.

[30] Li Jun MA, Zhan J and Zhang HQ. Recent progress in patient-derived tumor xenograft model of breast cancer. Scientia Sinica 2016.

[31] Tang LH, Gonen M, Hedvat C, Modlin IM and Klimstra DS. Objective quantification of the Ki67 proliferative index in neuroendocrine tumors of the gastroenteropancreatic system: a comparison of digital image analysis with manual methods. Am J Surg Pathol 2012; 36: 1761-1770.

[32] Klimowicz AC, Bose P, Petrillo SK, Magliocco AM, Dort JC and Brockton NT. The prognostic impact of a combined carbonic anhydrase IX and Ki67 signature in oral squamous cell carcinoma. Br J Cancer 2013; 109: 1859-1866.

[33] Lopez F, Belloc F, Lacombe F, Dumain P, Reiffers J, Bernard P and Boisseau MR. Modalities

of synthesis of Ki67 antigen during the stimulation of lymphocytes. Cytometry 1991; 12: 42-49.

[34] Macdonald J, Henri J, Goodman L, Xiang D, Duan W and Shigdar S. Development of a bifunctional aptamer targeting the transferrin receptor and epithelial cell adhesion molecule (EpCAM) for the treatment of brain cancer metastases. ACS Chem Neurosci 2017; 8: 777-784.

[35] Meng Y, Xu BQ, Fu ZG, Wu B, Xu B, Chen ZN and Li L. Cytoplasmic EpCAM over-expression is associated with favorable clinical outcomes in pancreatic cancer patients with Hepatitis B virus negative infection. Int J Clin Exp Med 2015; 8: 22204-22216.

[36] Fong D, Seeber A, Terracciano L, Kasal A, Mazzoleni G, Lehne F, Gastl G and Spizzo G. Expression of EpCAM(MF) and EpCAM(MT) variants in human carcinomas. J Clin Pathol 2014; 67: 408-414.

[37] Yonaiyama S, Toyoki Y, Morohashi S, Sakuraba S, Yoshizawa T, Suzuki T, Wu Y, Kijima H and Hakamada K. Epithelial cell adhesion molecule (EpCAM) overexpression is correlated with malignant potentials of intraductal papillary mucinous neoplasms (IPMNs) of the pancreas. Biomed Res 2013; 34: 87-95.

[38] Abd El-Maqsoud NM and Abd El-Rehim DM. Clinicopathologic implications of EpCAM and Sox2 expression in breast cancer. Clin Breast Cancer 2014; 14: e1-9.

[39] Zhou B, Der CJ and Cox AD. The role of wild type RAS isoforms in cancer. Semin Cell Dev Biol 2016; 58: 60-69.

[40] Bournet B, Muscari F, Guimbaud R, Cordelier P and Buscail L. KRAS mutations and their correlation with survival of patients with advanced pancreatic cancer. Pancreas 2013; 42: 543-544.

[41] Cicenas J, Kvederaviciute K, Meskinyte I, Meskinyte-Kausiliene E, Skeberdyte A and Cicenas J. KRAS, TP53, CDKN2A, SMAD4, BRCA1, and BRCA2 mutations in pancreatic cancer. Cancers (Basel) 2017; 9.

[42] Potula R, Haorah J, Knipe B, Leibhart J, Chrastil J, Heilman D, Dou H, Reddy R, Ghorpade A and Persidsky Y. Alcohol abuse enhances neuroinflammation and impairs immune responses in an animal model of human immunodeficiency virus-1 encephalitis. Am J Pathol 2006; 168: 1335-1344.